Quantum computation and error correction based on continuous variable cluster states

Shuhong Hao(郝树宏), Xiaowei Deng(邓晓玮), Yang Liu(刘阳), Xiaolong Su(苏晓龙), Changde Xie(谢常德), and Kunchi Peng(彭堃墀)

Citation: Chin. Phys. B, 2021, 30 (**6**): 060312. DOI: 10.1088/1674-1056/abeb0a
Journal homepage: http://cpb.iphy.ac.cn; http://iopscience.iop.org/cpb

What follows is a list of articles you may be interested in

Quantum computation and simulation with vibrational modes of trapped ions

Wentao Chen(陈文涛), Jaren Gan, Jing-Ning Zhang(张静宁), Dzmitry Matuskevich, and Kihwan Kim(金奇奂)
Chin. Phys. B, 2021, 30 (**6**): 060311. DOI: 10.1088/1674-1056/ac01e3

Efficient self-testing system for quantum computations based on permutations

Shuquan Ma(马树泉), Changhua Zhu(朱畅华), Min Nie(聂敏), and Dongxiao Quan(权东晓)
Chin. Phys. B, 2021, 30 (**4**): 040305. DOI: 10.1088/1674-1056/abe29a

Taking tomographic measurements for photonic qubits 88 ns before they are created

Zhibo Hou(侯志博), Qi Yin(殷琪), Chao Zhang(张超), Han-Sen Zhong(钟翰森), Guo-Yong Xiang(项国勇), Chuan-Feng Li(李传锋), Guang-Can Guo(郭光灿), Geoff J. Pryde, and Anthony Laing
Chin. Phys. B, 2021, 30 (**4**): 040304. DOI: 10.1088/1674-1056/abe29c

Realization of arbitrary two-qubit quantum gates based on chiral Majorana fermions

Qing Yan(闫青) and Qing-Feng Sun(孙庆丰)
Chin. Phys. B, 2021, 30 (**4**): 040303. DOI: 10.1088/1674-1056/abe296

Nonlocal advantage of quantum coherence in a dephasing channel with memory

Ming-Liang Hu(胡明亮), Yu-Han Zhang(张宇晗), and Heng Fan(范桁)
Chin. Phys. B, 2021, 30 (**3**): 030308. DOI: 10.1088/1674-1056/abcf4a

---

TOPICAL REVIEW — Quantum computation and quantum simulation

Quantum computation and error correction based on continuous variable cluster states*

Shuhong Hao(郝树宏)[1,2], Xiaowei Deng(邓晓玮)[1,3], Yang Liu(刘阳)[1,3], Xiaolong Su(苏晓龙)[1,†], Changde Xie(谢常德)[1], and Kunchi Peng(彭堃墀)[1]

[1] State Key Laboratory of Quantum Optics and Quantum Optics Devices, Collaborative Innovation Center of Extreme Optics, Institute of Opto-Electronics, Shanxi University, Taiyuan 030006, China

[2] School of Mathematics and Physics, Anhui University of Technology, Maanshan 243000, China

[3] Shenzhen Institute for Quantum Science and Engineering, Southern University of Science and Technology, Shenzhen 518055, China

(Received 26 November 2020; revised manuscript received 17 February 2021; accepted manuscript online 2 March 2021)

Measurement-based quantum computation with continuous variables, which realizes computation by performing measurement and feedforward of measurement results on a large scale Gaussian cluster state, provides a feasible way to implement quantum computation. Quantum error correction is an essential procedure to protect quantum information in quantum computation and quantum communication. In this review, we briefly introduce the progress of measurement-based quantum computation and quantum error correction with continuous variables based on Gaussian cluster states. We also discuss the challenges in the fault-tolerant measurement-based quantum computation with continuous variables.

Keywords: quantum computation, quantum error correction, continuous variables, cluster state

PACS: 03.67.−a, 03.67.Mn, 42.50.−p **DOI:** 10.1088/1674-1056/abeb0a

1. Introduction

Quantum computation (QC) provides an exponential speedup over classical computing for certain problems, such as integer factoring[1] and quantum simulation.[2] Recently, quantum computation with several systems, such as superconducting systems,[3–5] ion trap systems,[6] and silicon-based systems,[7] has made enormous progress. Generally, there are two kinds of QC models, one is the traditional circuit model, in which unitary evolution and coherent control of individual qubits are required,[8] the other one is the measurement-based QC model,[9] which is also named one-way QC since computation is implemented by performing measurement and feedforward of measurement results on a large scale cluster state. The measurement-based QC is scalable and provides the ability to perform universal QC using only single-qubit projective measurement, given a specially prepared and highly entangled cluster state.[9,10] In the measurement-based QC, the resources required for QC using linear optics can be significantly reduced by first creating photonic cluster states via nondeterministic gates.[10] Essential progress has been made for measurement-based QC, such as measurement-based QC with a four-qubit cluster state of single photons[11–13] and measurement-based quantum computation with trapped ions system.[14]

To build a quantum computer, seven stages are involved,[15] which are (1) operations on single physical qubits, (2) algorithms on multiple physical qubits, (3) quantum nondemolition (QND) measurements for error correction and control, (4) logical memory with longer lifetime than that of physical qubits, (5) operations on single logical qubits, (6) algorithms on multiple logical qubits, and (7) fault-tolerant quantum computation. These stages are divided according to the complexity of the task and different technologies are required at each stage. At present, the third stage has been attained by trapped ions[16] and superconducting system,[17] respectively. The fourth stage, where a logical qubit can be stored, via error correction, for a time substantially longer than the decoherence time of its physical qubit components, has not been reached. Recently, quantum states on 53 qubits were created using a programmable superconducting process[18] and Gaussian boson sampling was demonstrated using 50 single-mode squeezed states.[19]

For quantum information based on optical systems, there are two different systems, which are discrete variable (DV) and continuous variable (CV) systems, respectively. Quantum variables defined in finite and infinite Hilbert spaces are used in DV and CV systems, respectively. Optical quantum information with DV and CV systems are developing in parallel and have their own advantages and disadvantages. The DV system encodes information on discrete variables, such as polarization of photons. For the DV optical system, the maximal entanglement can be obtained but the generation of

*Project supported by the National Natural Science Foundation of China (Grant Nos. 11834010, 11804001, and 11904160), the Natural Science Foundation of Anhui Province, China (Grant No. 1808085QA11), the Program of Youth Sanjin Scholar, National Key R&D Program of China (Grant No. 2016YFA0301402), and the Fund for Shanxi "1331 Project" Key Subjects Construction.

†Corresponding author. E-mail: suxl@sxu.edu.cn

entanglement is probabilistic usually. While for the CV optical system, which always encodes information on the amplitude and phase quadratures (corresponding to position and momentum, respectively) of an optical field, the generation of entanglement is deterministic but the perfect entanglement is not able to be obtained.[20,21] So far, tremendous progress has been achieved for optical quantum networks with DV and CV systems.

Cluster state is the basic resource for measurement-based QC. There has been remarkable achievement in the preparation of CV cluster state, from four-mode[22–24] to eight-mode,[25] 60-mode in frequency comb,[26] 10000-mode,[27] one million modes,[28] and two-dimensional one in time domain.[29,30] The successful preparation of large scale CV cluster state makes it possible to realize the measurement-based QC with CV cluster state. Measurement-based QC with CV cluster states provides a feasible way for scalable quantum information processing.[9,10] It can be realized by measurement and classical feedforward on a Gaussian cluster state, which is prepared deterministically.[21,31,32] Firstly, a quantum nondemolition sum gate and a quadratic phase gate for measurement-based CV QC were demonstrated based on utilizing squeezed states of light in 2008 and 2009, respectively.[33,34] Successively, a controlled-X gate based on a four-mode CV cluster state was presented, in which a pair of quantum teleportation elements were used for the transformation of quantum states from the input target and control states to the output states.[35] Later, the squeezing operation, Fourier transformation, and controlled-phase gate were also achieved, in which a four-mode optical cluster states served as the resource quantum states.[36,37] Currently, several quantum logical gates in CV QC have been demonstrated, but the realization of an algorithm remains a challenge.

In the practical QC, the inevitable interaction between the quantum state and environment will lead to errors. Thus, quantum error correction (QEC) is a necessary procedure to protect quantum state against errors. The essential idea in QEC is to encode information in subsystems of a larger physical space that are immune to noise.[3] In QEC, physical qubits are encoded as QEC code, which is used to identify errors and correct the corresponding errors. In fault-tolerant QC, logical qubits are encoded within the error-corrected system of physical qubits and are used to implement quantum algorithms.[3] In recent years, proof-of-principle experiments have been demonstrated in various experimental systems.[16,17,38–41] Fault-tolerant QC, which implements QC by encoding quantum states in a QEC code, enables one to build a quantum computer which behaves correctly in the presence of errors.[42,43] Fault-tolerant measurement-based QC with CV cluster states is possible with finite squeezed cluster states above a threshold value by concatenating with quantum stabilizer codes and some special ancilla-based quantum code such as Gottesman–Kitaev–Preskill (GKP) code.[44]

In this paper, we briefly introduce the progress of CV measurement-based QC. In Section 2, the progress of Gaussian cluster state, the theoretical principle of measurement-based CV QC, the experimental details of the related techniques, and the applications of some CV quantum logical gates are introduced. In Section 3, we introduce the progress of CV quantum simulation. In Section 4, the progress of CV QEC, the fault-torrent measurement-based quantum computation with two classes of QEC codes and the recent progress of the experiment techniques are introduced. Finally, we discuss the challenges toward fault-tolerant CV QC.

2. Measurement-based CV QC

2.1. The CV cluster state

Cluster state, which is a type of multipartite entangled state with next-neighbor interactions (Ising type interactions),[32,45] is the basic resource for measurement-based QC[9,10] and quantum network.[46,47] In CV QC, the quantum variables are the amplitude and phase quadratures of the quantum electromagnetic field described as $\hat{a}$, which satisfies the usual bosonic commutator $[\hat{a},\hat{a}^{\dagger}]=1$. When the convention $\hbar=1/2$ is chosen, its amplitude and phase quadratures can be expressed as $\hat{x}=(\hat{a}+\hat{a}^{\dagger})/2$ and $\hat{p}=\left(\hat{a}-\hat{a}^{\dagger}\right)/2\mathrm{i}$, respectively. The variance of the vacuum state is given by $\sigma(\hat{x})^2=\sigma(\hat{p})^2=1/4$. Generally, CV cluster states are defined as

$$\hat{p}_a-\sum_{b\in N_a}\hat{x}_b\equiv\hat{\delta}_a\to 0,\quad a\in G. \tag{1}$$

The modes $a\in G$ denote the vertices of the graph G, while the modes $b\in N_a$ are the next-neighbors of mode $\hat{a}$ for ideal case, the excess noise $\hat{\delta}_a$ tends to be zero.

As shown in Fig. 1, each node in a cluster state represents a qubit or qumode, the edge represents the next-neighbor interaction between the neighboring nodes.[32] It is obvious that the cluster state can protect entanglement property since when a measurement is performed on one qubit or qumode only the interaction next to this qubit is destroyed, while the entanglement of other qubits not next to the measured qubit still exists.[48] Based on this entanglement persistence property, the cluster state is a naturally good resource for measurement-based QC.[9,10]

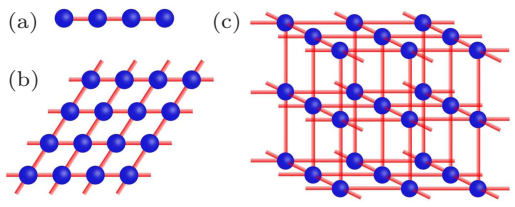

Fig. 1. Examples of cluster states. (a) A linear four-mode cluster state. (b) A two-dimensional cluster state. (c) A three-dimensional cluster state.

There are mainly three types of experimentally prepared CV cluster states, which are space-separated, frequency-domain, and time-domain cluster states, respectively. These three types of CV cluster states are developing in parallel and have their own advantages and disadvantages. To prepare the space-separated CV cluster state, a linear optical transformation of squeezed states on a specially designed beam-splitter network is used.[22–25] The advantage of the space-separated cluster state is that local operations can be easily applied to each qumode. The drawback of this method is that with increasing of the entangled modes the complexity of the experimental setup is also subsequently increased. Using this method, space-separated four-mode and eight-mode CV cluster states were prepared experimentally[22–25] and applied in CV QC, respectively.

To prepare the CV cluster state in frequency domain, the technique of the optical frequency comb is applied, with which the lager scale cluster states can be prepared in principle.[49] In 2014, Chen *et al.* experimentally realized one 60-mode copy and of two 30-mode copies of a dual-rail quantum-wire cluster state in the quantum optical frequency comb of a bimodally pumped optical parametric oscillator.[26] In 2017, Cai *et al.* realized the construction of thirteen cluster states by measuring a frequency comb with appropriate pulse shaped local oscillator, which was obtained by a computer-programmed spatial light modulator.[50] However, in this way, these entangled modes are not easily separated and thus the schemes of utilizing them to implement QC need to be redesigned.

To prepare the CV cluster state in time domain, two squeezed light beams are divided into time bins and are coupled on a balanced beamsplitter.[27] Then one output mode from the balanced beamsplitter is delayed through a fibre delay line. Finally, by combining the staggered states on the second balanced beamsplitter, a cluster state in time domain can be generated.[27] In 2016, Yoshikawa *et al.* demonstrated the successive generation of fully inseparable light modes for more than one million modes.[28] Remarkably, in 2019, two-dimensional cluster states were experimentally prepared by Furusawa's group and Anderson's group, respectively.[29,30] Very recently, a method to generate CV three-dimensional cluster state in time domain was proposed for topologically-protected measurement-based QC.[51] It has been shown that such a three-dimensional cluster state is robust against analog errors derived from the finite squeezing during topologically protected measurement-based QC.

2.2. The CV measurement-based QC

The CV measurement-based QC is based on the cluster entangled state, which can be built by implementing an appropriate unitary transformation on a series of input squeezing state.[52] The elementary gate set which is sufficient for universal CV QC of arbitrary multi-qumode can be chosen as[10,53–55]

$$\{F, D_{1,\hat{x}}(s), D_{2,\hat{x}}(s), D_{3,\hat{x}}(s), C_z\}. \tag{2}$$

Here $F = \mathrm{e}^{-\mathrm{i}(\pi/2)\hat{a}\hat{a}^\dagger}$ is the Fourier transformation operator,[56] which maps between the position and momentum basis states. $D_{k,\hat{x}}(s) = \exp(\mathrm{i}s\hat{x}^k/k)$, for $k = 1,2,3$ and for all $s \in R$. For example, $D_{1,\hat{x}}(s) = \exp(\mathrm{i}s\hat{x})$ and $D_{1,\hat{p}}(s) = \exp(-\mathrm{i}s\hat{p})$ are displacement gates which displace a state in phase space by s in $\hat{x}$ and $\hat{p}$, respectively. $D_{2,\hat{x}}(s)$ is the quadratic phase gate (shear gate), and $D_{3,\hat{x}}(s)$ is the cubic phase gate, which is the single nonlinear non-Gaussian gate. $C_Z = \mathrm{e}^{\mathrm{i}\hat{x}_1\otimes\hat{x}_2}$ is the controlled-Z gate, which describes the two-mode logical gate. The quadratic phase gate $D_{2,\hat{x}}(s)$ together with F, $D_{1,\hat{x}}(s)$, and C_Z is sufficient to simulate any multiqumode Clifford (Gaussian) transformation. In order to asymptotically achieve universal multi-qumode processing including non-Clifford (non-Gaussian) unitaries, the additional cubic phase gate $D_{3,\hat{x}}(s)$ is needed.[54]

A Gaussian state can be described by using the covariance matrix, which is defined as $\mathrm{cov}(\hat{\boldsymbol{v}})_{ij} = \frac{1}{2}\langle \hat{\boldsymbol{v}}_i\hat{\boldsymbol{v}}_j + \hat{\boldsymbol{v}}_j\hat{\boldsymbol{v}}_i\rangle - \langle\hat{\boldsymbol{v}}_i\rangle\langle\hat{\boldsymbol{v}}_j\rangle$, $i,j = 1,2,3,\ldots,n$, where $\hat{\boldsymbol{v}} = (\hat{x}_1,\hat{p}_1,\ldots,\hat{x}_n,\hat{p}_n)^{\mathrm{T}}$ is a vector composed by the quadrature operators.[57] In quantum optics, the Hamiltonians with quadratic $\hat{x}$ and $\hat{p}$ can be written as $\hat{U} = \exp[\mathrm{i}\sum_{j,k}(\alpha_{j,k}\hat{x}_j\hat{x}_k + \beta_{j,k}\hat{x}_j\hat{p}_k + \gamma_{j,k}\hat{p}_j\hat{p}_k) + \mathrm{i}\sum_j(\delta_j\hat{x}_j + \varepsilon_j\hat{p}_j) + \mathrm{i}\phi]$, $\alpha_{j,k},\beta_{j,k},\gamma_{j,k},\delta_j,\varepsilon_j,\ \phi \in R$, which transforms Gaussian states into Gaussian states and is called as Gaussian transformation or linear unitary Bogoliubov (LUBO) transformation.[56] After this transformation, we get $\hat{U}^\dagger\hat{\boldsymbol{v}}\hat{U} = L\hat{\boldsymbol{v}} + \boldsymbol{c}$, $\mathrm{Det}(L) = 1$, where L is a $2n\times 2n$ symplectic matrix and $\boldsymbol{c}$ is a vector of $2n$ constants. The effect of the Gaussian transformation L to a special Gaussian state $\hat{\boldsymbol{v}}_0$ can be described as $\mathrm{cov}\hat{\boldsymbol{v}} = \mathrm{cov}(L\hat{\boldsymbol{v}}_0) = L(\mathrm{cov}\hat{\boldsymbol{v}}_0)L^{\mathrm{T}}$. For example, the symplectic matrices of the Fourier transformation operator, the quadratic phase gate, and the controlled-Z gate are given respectively by

$$F = \begin{pmatrix} 0 & -1 \\ 1 & 0 \end{pmatrix}, \tag{3}$$

$$D_{2,\hat{x}} = \begin{pmatrix} 1 & 0 \\ s & 1 \end{pmatrix}, \tag{4}$$

$$C_z = \begin{pmatrix} 1 & 0 & 0 & 0 \\ 0 & 1 & 1 & 0 \\ 0 & 0 & 1 & 0 \\ 1 & 0 & 0 & 1 \end{pmatrix}. \tag{5}$$

Measurement-based QC is realized by measurement and classical feedforward based on cluster state.[9,10] An arbitrary one-mode Gaussian logical gate can be exactly and finitely decomposed into the elementary logical gates, such as the quadratic phase gate and the Fourier transformation gate.[56] Here we take $D_{2,\hat{x}}(s)$ as an example to present the basic principle of the measurement-based CV QC. As shown in Fig. 2, the initial input state $|\Psi_{\mathrm{in}}\rangle$ is coupled with a momentum eigenstate with eigenvalue zero $|0\rangle_p = (2\pi)^{-1/2}\int \mathrm{d}\hat{x}|\hat{x}\rangle_x$, which is

an ideal phase squeezed state $\hat{a} = \mathrm{e}^{+r}\hat{x}^{(0)} + \mathrm{i}\,\mathrm{e}^{-r}\hat{p}^{(0)}$. After the coupling by a controlled-Z gate, one of the output modes is measured by a homodyne detector (HD) to obtain the quadrature of $\hat{p}' = \hat{p}\cos\theta - \hat{x}\sin\theta$. Then the measurement result is fedforward to the other output mode with the gain of $g = 1/\cos\theta$ and $\theta = \tan^{-1}(-s)$ by the amplitude quadratures displacement operation $D_{1,\hat{p}}(s) = \exp(-\mathrm{i}s\hat{p})$. After the displacement operation, the quadratic phase gate is realized. Usually, the controlled-Z gate illustrated in Fig. 2 is implemented by a beamsplitter operation in the experiment.[37,58]

In 2011, Ukai *et al.* demonstrated the complete set of one-mode linear unitary Bogoliubov (LUBO) transformations for continuous variables using a four-mode cluster state.[56] The fidelity obtained in the experiment was 0.68, which was limited by the squeezing level of the ancillary cluster state. In 2014, Hao *et al.* experimentally realized single-mode squeezing and Fourier transformation operations by using an Einstein–Podolsky–Rosen (EPR) entangled state as the resource.[58] The fidelity of the squeezing operation was 0.65 for 4 dB squeezing operation, which was limited by the squeezing level of the EPR entangled state. In 2016, Marshall *et al.* experimentally demonstrated the CV QC on encrypted data with Gaussian displacement and squeezing operations which can protect the security of a user's privacy.[59] The fidelity was $> 97\%$ for losses of up to 10 km. In 2017, a scheme to realize a general single-mode Gaussian operation based on an EPR entangled state was proposed[60] and it has been shown that the classical Hadamard transform algorithm can be implemented with CV cluster state.[61] In 2020, Zhao *et al.* proposed and experimentally demonstrated a heralded squeezing gate which achieved near unit fidelity for coherent inputs while requiring only modest ancillary squeezing and post-selection filter.[62]

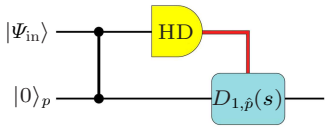

Fig. 2. Schematic diagram of the elementary one-mode measurement-based QC gate. $|\Psi_{\rm in}\rangle$ is the input state, $|0\rangle_p$ is a momentum eigenstate with eigenvalue zero, HD is a homodyne detection in the phase quadrature, and $D_{1,\hat{p}}(s)$ is a correction displacement operator.

To realize a two-mode logical gate, such as controlled-Z gate and controlled-X ($C_X = \mathrm{e}^{\mathrm{i}\hat{x}_1\otimes\hat{p}_2}$) gate, two input states are coupled with a four-mode cluster state and two quantum teleportation circuits need to be implemented. In 2010, Wang *et al.* demonstrated a controlled-X gate based on a four-mode CV cluster state of optical modes.[35] In 2011, Ukai *et al.* demonstrated a CV cluster-based C_Z gate.[37] To realize universal CV QC based on cluster state, at least one non-Gaussian operation is required, for example the cubic phase gate $D_{3,\hat{x}}(s)$, besides Gaussian cluster state and Gaussian measurement.[10]

2.3. Experimental realization of the logical gates for CV QC

In the experiment, the amplitude (or phase) quadrature displacement operation $D_{1,\hat{x}}(s))$ (or $D_{1,\hat{p}}(s)$) can be realized by coupling the input mode with a coherent beam on a 99 : 1 beam splitter.[54] The displacement amplitude can be controlled by the electro-optical modulators (EOM) placed in the coherent beam. The phase rotation operator $\hat{R}(\theta) = \mathrm{e}^{-\mathrm{i}\theta\hat{a}\hat{a}^\dagger}$ whose symplectic matrix is given by

$$R(\theta) = \begin{pmatrix} \cos\theta & \sin\theta \\ -\sin\theta & \cos\theta \end{pmatrix}, \tag{6}$$

can be considered as the control of the phase of the input state. So we can lock the relative phase between two optical beams to implement the rotation operation. Fourier transform is the special case of rotation operation when $\theta = \pi/2$.

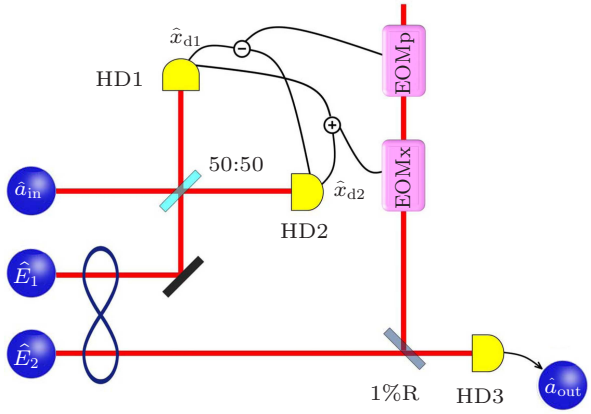

Fig. 3. The schematic of experimental setup of a squeezing gate. The sum $(+)$ and difference $(-)$ of the photocurrents measured by two homodyne detectors (HD1 and HD2) are fedforward to mode $\hat{E}_2$. The output mode is measured by HD3. EOMx and EOMp are the amplitude and phase electro-optical modulators. 1%R is a mirror with a 1% reflection coefficient. Revised from Fig. 1 in Ref. [58].

Squeezing operation and Fourier transform have been efficiently realized based on EPR entangled state.[58] The schematic of experimental setup of a squeezing gate is shown in Fig. 3. The quantum correlations for amplitude and phase quadratures of the EPR entangled state are $\hat{x}_1 + \hat{x}_2 \equiv \hat{\delta}_1$ and $\hat{p}_1 - \hat{p}_2 \equiv \hat{\delta}_2$, respectively, where $\hat{\delta}_1$ and $\hat{\delta}_2$ represent excess noises with variances of $\sigma(\hat{\delta}_1)^2 = \sigma(\hat{\delta}_2)^2 = \mathrm{e}^{-2r_E}/4$ introduced by finite squeezing. For an ideal EPR entangled state (in case of infinite squeezing), we have $\hat{\delta}_1 = \hat{\delta}_2 = 0$. The input mode $\hat{a}_{\rm in}$ is coupled with the submode $\hat{E}_1$ by a 50 : 50 beam splitter with a $\pi/2$ phase difference. The coupled modes of the beam splitter are measured by two homodyne detectors HD_1 and HD_2, respectively. The measurement results $\hat{x}_{\rm d1}$ and $\hat{x}_{\rm d2}$ are given respectively by

$$\begin{aligned} \hat{x}_{\rm d1} &= [\cos\theta_1(\hat{x}_{\rm in} - \hat{p}_1) + \sin\theta_1(\hat{p}_{\rm in} + \hat{x}_1)]/\sqrt{2}, \\ \hat{x}_{\rm d2} &= [\cos\theta_2(\hat{x}_{\rm in} + \hat{p}_1) + \sin\theta_2(\hat{p}_{\rm in} - \hat{x}_1)]/\sqrt{2}, \end{aligned} \tag{7}$$

where θ_1 and θ_2 are the measurement angles of HD_1 and HD_2, respectively. Choose $\theta_2 = \theta_1$ and feed forward the measure-

ment results to the submode $\hat{E}_2$, which is implemented by coupling the displaced coherent beam and submode $\hat{E}_2$ on a beam splitter with reflectivity of 1%. The output state is given by

$$\begin{pmatrix} \hat{x}_{\rm out} \\ \hat{p}_{\rm out} \end{pmatrix} = \begin{pmatrix} \hat{x}_2 \\ \hat{p}_2 \end{pmatrix} + G_{\rm s} \begin{pmatrix} \hat{x}_{\rm d1} \\ \hat{x}_{\rm d2} \end{pmatrix} = L \begin{pmatrix} \hat{x}_{\rm in} \\ \hat{p}_{\rm in} \end{pmatrix} + \boldsymbol{\delta}, \quad (8)$$

where $G_{\rm s}$ is the gain factor in the feedforward circuit, which can be described as

$$G_{\rm s} = \begin{pmatrix} \dfrac{1}{\sqrt{2}\sin\theta_1} & \dfrac{1}{\sqrt{2}\sin\theta_1} \\ \dfrac{1}{\sqrt{2}\cos\theta_1} & \dfrac{-1}{\sqrt{2}\cos\theta_1} \end{pmatrix}, \quad (9)$$

L is the transformation matrix of the squeezing gate

$$L = \begin{pmatrix} \cot\theta_1 & 0 \\ 0 & \tan\theta_1 \end{pmatrix}, \quad (10)$$

and $\boldsymbol{\delta} = (\hat{\delta}_1, -\hat{\delta}_2)^{\rm T}$ is the excess noise coming from the EPR entangled state.

The standard squeezing gate $\hat{S}(r) = {\rm e}^{{\rm i}r(\hat{x}\hat{p}+\hat{p}\hat{x})}$, whose transformation matrix is

$$S = \begin{pmatrix} {\rm e}^{r} & 0 \\ 0 & {\rm e}^{-r} \end{pmatrix}. \quad (11)$$

Comparing the matrixes of L and S, we can see that the squeezing gate can be obtained when ${\rm e}^{r} = \cot\theta_1$ and the squeezing parameter r depends on the measurement angle θ_1.

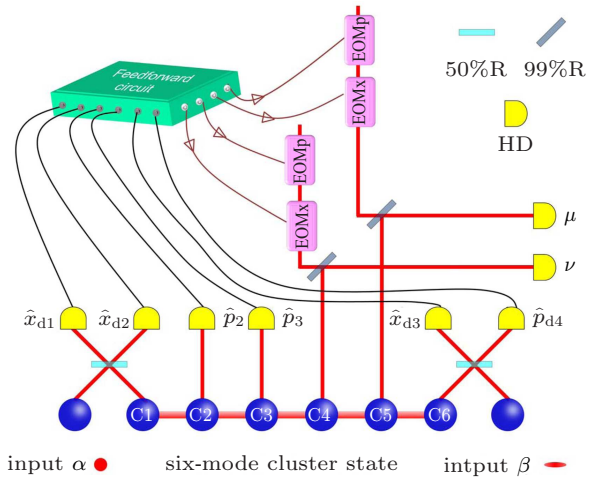

Fig. 4. Schematic of experimental setup of the gate sequence. The input states α and β are coupled to a six-mode CV cluster state via two 50 : 50 beam-splitters, respectively. Measurement results from HD systems are fedforward to modes C4 and C5. The output modes μ and ν are measured by two HD systems. EOMx and EOMp: amplitude and phase EOM. 99%R, a mirror with 99% reflection coefficient. Revised from Fig. 3 in Ref. [63].

Arbitrary Gaussian QC can be implemented sufficiently by a sequence of one-mode and two-mode logical gates. Here, a gate sequence consisting of a one-mode squeezing gate $\hat{S}(r_s) = {\rm e}^{{\rm i}r_s(\hat{x}\hat{p}+\hat{p}\hat{x})}$ and a two-mode controlled-Z gate $\hat{C}_{Zjk} = {\rm e}^{2{\rm i}\hat{x}_j\hat{x}_k}$ based on a six-mode CV cluster state is taken as an example.[63]

As shown in Fig. 4, the input mode α (target mode) and the other input mode β (control mode) are coupled with the sub-mode C1 and C6 of the six-mode cluster state by 50 : 50 beam splitters, respectively. In the experiment, the amplitude and phase quadratures $\hat{x}_{\rm d1}, \hat{x}_{\rm d2}$, $\hat{x}_{\rm d3}$, and $\hat{p}_{\rm d4}$ of the output modes of two 50 : 50 beam splitters are measured by homodyne detectors, respectively, where the measurement angles θ_1 and θ_2 in the homodyne detection for $\hat{x}_{\rm d1}$ and $\hat{x}_{\rm d2}$ determine the squeezing operation. The other two phase quadratures $\hat{p}_2$ and $\hat{p}_3$ coming from the sub-modes $C2$ and $C3$ of the six-mode cluster state are also measured. These measured results are fedforward to the amplitude and phase quadratures of modes $C4$ and $C5$ through classical feedforward circuits by using the amplitude and phase EOM, respectively. In this way, the squeezing gate on input mode α is performed firstly to produce a phase-squeezed state. Then a C_Z gate is performed on the output mode from the squeezing gate and the other input mode β coming from outside of the sequence. The whole gate sequence is described as

$$\begin{aligned} \begin{pmatrix} \hat{x}_\mu \\ \hat{p}_\mu \\ \hat{x}_\upsilon \\ \hat{p}_\upsilon \end{pmatrix} &= \begin{pmatrix} \hat{x}_{C4} \\ \hat{p}_{C4} \\ \hat{x}_{C5} \\ \hat{p}_{C5} \end{pmatrix} + G \begin{pmatrix} \hat{p}_3 - \csc\theta_2(\hat{x}_{\rm d1} + \hat{x}_{\rm d2})/\sqrt{2} \\ \hat{p}_2 + \sec\theta_2(\hat{x}_{\rm d1} - \hat{x}_{\rm d2})/\sqrt{2} \\ \sqrt{2}\hat{x}_{\rm d3} \\ \sqrt{2}\hat{p}_{\rm d4} \end{pmatrix} \\ &= U \begin{pmatrix} \hat{x}_\alpha \\ \hat{p}_\alpha \\ \hat{x}_\beta \\ \hat{p}_\beta \end{pmatrix} + \begin{pmatrix} \hat{\delta}_1 - \hat{\delta}_3 \\ \hat{\delta}_4 - \hat{\delta}_2 - \hat{\delta}_6 \\ -\hat{\delta}_6 \\ \hat{\delta}_1 + \hat{\delta}_5 - \hat{\delta}_3 \end{pmatrix}, \end{aligned} \quad (12)$$

where

$$G = \begin{pmatrix} -1 & 0 & 0 & 0 \\ 0 & -1 & 1 & 0 \\ 0 & 0 & 1 & 0 \\ -1 & 0 & 0 & 1 \end{pmatrix} \quad (13)$$

is the feedforward gain factor, and

$$U = \begin{pmatrix} 1 & 0 & 0 & 0 \\ 0 & 1 & 1 & 0 \\ 0 & 0 & 1 & 0 \\ 1 & 0 & 0 & 1 \end{pmatrix} \begin{pmatrix} \cot\theta_2 & 0 & 0 & 0 \\ 0 & \tan\theta_2 & 0 & 0 \\ 0 & 0 & 1 & 0 \\ 0 & 0 & 0 & 1 \end{pmatrix} \quad (14)$$

is the transformation matrix of the gate sequence. $\hat{\delta}_i$ $(i = 1, 2, \ldots, 6)$ are the corresponding excess noise terms for each mode of the CV six-mode linear cluster state. The quantum property of this gate sequence is confirmed by the fidelities and the quantum entanglement of the two output modes, which depend on both the squeezing and controlled-phase gates.[63] This experiment demonstrates the feasibility of implementing Gaussian quantum computation by means of accessible gate sequences.

2.4. Non-Gaussian gate for CV QC

Non-Gaussian gate is a key part in CV QC for exponential speedup to solve certain computational problems.[54] Bosonic operators of annihilation $\hat{a}$ and creation $\hat{a}^\dagger$ are essential non-Gaussian operations. The annihilation operation

can be realized by transmitting the target state through a low reflectivity beam splitter. Once a single photon in the reflection channel is detected, it can be treated that the annihilation operation is conditionally realized.[64,65] Photon creation operation can also be conditionally achieved with the help of a low-amplitude spontaneous parametric down-conversion progress.[64,65]

It has been shown that in order to achieve arbitrary unitary operations for CV QC, it is essential to add a cubic gate to other Gaussian operations.[55] Gottesman, Kitaev, and Preskill proposed a scheme to realize a cubic gate with Gaussian operations, Gaussian measurement, quadratic feedforward, and an ancillary cubic state, which is based on the two-mode squeezed vacuum and photon number resolving detectors.[66] In 2011, Marek *et al.* proposed a scheme to achieve weak nonlinearity with single-mode squeezed vacuum state and photon subtraction or addition technique.[67] In 2015, Marshall *et al.* introduced a "repeat-until-success" approach to generate the cubic phase gate by using sequential photon subtractions and Gaussian operations.[68] In 2016, Miyata *et al.* presented the implementation of a quantum cubic gate by an adaptive non-Gaussian measurement which composed of a non-Gaussian ancillary state, linear optics, and adaptive heterodyne measurement.[69] In this scheme, the nonlinearity is generated by a classical nonlinear adaptive control in a measurement-and-feedforward process, while the nonclassicality is obtained by the cubic state.

Non-Gaussian ancilla is important to complete the cubic phase gate. It has been shown that the weak cubic nonlinearity can be prepared within reach of current technologies.[70] The nonclassicality of the approximative weak cubic state lies in the superposition of $|1\rangle$ and $|3\rangle$. So, it can be heralded prepared as a superposition of Fock states. In detail, the idler mode from an entangled two-mode squeezed state is split into three by a pair of beam splitters, after which the states of the three modes are displaced in phase space. Simultaneous detection of a photon by the three detectors then heralds approximative preparation of the superposition state in the signal mode.

3. CV quantum simulation

Quantum simulation enables one to mimic the evolution of other quantum systems using a controllable quantum system.[71–74] A CV quantum computer may be more suitable for simulating CV quantum systems.[75] A scheme for simulating the Kitaev lattice model and detecting statistics of Abelian anyons is proposed, where a quadratic phase gate is used to detect the important feature of anyons, that is the nontrivial statistical phase obtainable through braiding.[76] In 2015, a quantum simulation scheme of quantum field theory using continuous variables was proposed.[77] Huh *et al.* proposed a quantum simulation scheme with modification of boson sampling, in which squeezed states of light are coupled to a boson sampling optical network to simulate the molecular vibronic spectra.[78] In 2018, Arrazola and Bromley showed that Gaussian boson sampling is a useful tool for dense subgraph identification.[79] In the same year, Brádler *et al.* proposed a method to estimate the number of perfect matchings of undirected graphs based on the relation between Gaussian boson sampling and graph theory.[80] Very recently, Gaussian boson sampling was experimentally demonstrated using 50 single-mode squeezed states as the input states,[19] which shows the advantage of QC. In the experiment, 50 indistinguishable single-mode squeezed states are sent into a 100-mode ultralow-loss interferometer with full connectivity and random matrix. The output states are sampled using 100 high-efficiency single-photon detectors, and the average fidelities around 0.99 are achieved in the experiment.

The experimental demonstration of CV quantum simulation is in progress. For example, quantum simulation for time evolution of quantum harmonic oscillators has been experimentally demonstrated by Deng *et al.*[81] According to the Hamiltonian of a quantum harmonic oscillator $\hat{H} = \hbar\omega(\hat{a}^{\dagger}\hat{a} + 1/2)$ in an open system with vacuum environment, the time evolution of the dimensionless position and momentum operators is given by

$$\begin{pmatrix} \hat{x}(t) \\ \hat{p}(t) \end{pmatrix} = \begin{pmatrix} \cos\omega t & \sin\omega t \\ -\sin\omega t & \cos\omega t \end{pmatrix} \left[\begin{pmatrix} \hat{x}(0)\,\mathrm{e}^{-Kt} \\ \hat{p}(0)\,\mathrm{e}^{-Kt} \end{pmatrix} + \begin{pmatrix} \hat{F}_x(t) \\ \hat{F}_p(t) \end{pmatrix} \right], \tag{15}$$

where K is the decay rate, and $\hat{F}_x(t)$ and $\hat{F}_p(t)$ are the noise operators depending on the reservoir variables.

Generally, the time evolution matrix can be mimicked using the rotation gate, while the interaction between the input state and vacuum environment resulting in the linear attenuation of the amplitude of the qumode can be mimicked by an adjustable beam-splitter composed by a half wave plate and a polarization beam-splitter. The rate of the attenuation is proportional to the strength of the interaction and the change of the interaction coefficient is mimicked by adjusting the transmittance $\sqrt{T} = \mathrm{e}^{-Kt}$ of the beam-splitter. The whole process is described as

$$\begin{aligned} \begin{pmatrix} \hat{x}_{\mathrm{out}} \\ \hat{p}_{\mathrm{out}} \end{pmatrix} = & \begin{pmatrix} \cos\theta & \sin\theta \\ -\sin\theta & \cos\theta \end{pmatrix} \left(\sqrt{T} \begin{pmatrix} \hat{x}_{\mathrm{in}} \\ \hat{p}_{\mathrm{in}} \end{pmatrix} + \sqrt{1-T} \begin{pmatrix} \hat{x}_{v} \\ \hat{p}_{v} \end{pmatrix} \right) \\ & + \begin{pmatrix} \hat{\delta}_1 \\ -\hat{\delta}_2 \end{pmatrix}. \end{aligned} \tag{16}$$

In the experiment, the Wigner function of the output state in phase space at different time points is measured to show the time evolution of a quantum harmonic oscillator in an open system for an initial coherent state and an initial amplitude-squeezed state, respectively. The measured fidelity, which is used for quantifying the quality of the simulation, is higher than its classical limit. This scheme may be used

to simulate more complicated dynamical processes of quantum systems, whose Hamiltonian is described by the position and momentum operators. Generally, the Hamiltonian of the simulated system can be decomposed into a set of unitary transformations,[82] so its dynamic behavior will possibly be simulated by a sequence of quantum logic operations in CV QC and the coupling of qu-modes. For example, the simulation of interaction between two bosonic oscillators with strong coupling[83] could be implemented by CV quantum simulation.

4. CV quantum error correction

QEC is a necessary procedure to protect quantum information against errors in QC.[3] In the framework of CV error correcting codes, one class generalizes qubit stabilizer codes which is referred as linear oscillator codes to a CV system.[84,85] This class falls in the Gaussian quantum information. The other class encodes a discrete system into a CV system and this class of codes requires using non-Gaussian states. A scalable fault-tolerant architecture can be obtained by concatenating these two classes of codes.[86]

In the regime of CV QEC, according to the no-go theorem for Gaussian QEC that Gaussian errors cannot be corrected by using only Gaussian resources.[87] However, non-Gaussian stochastic errors, which frequently occur in free-space channels with atmospheric fluctuations for example,[88,89] can be corrected by Gaussian schemes. Different types of CV QEC codes for correcting single non-Gaussian error have been proposed, such as nine-wave-packet code,[85,90] five-wave-packet code,[84,91] entanglement-assisted code,[92] and erasure-correcting code.[93] Some CV QEC schemes against displacement errors have been experimentally demonstrated, for example, the nine-wave-packet code,[94] the five-wave-packet code,[95] and the correcting code with the correlated noisy channels.[96] It has been shown that in fault-tolerant CV QC with cluster state, initial squeezing in the cluster above a threshold value of 20.5 dB ensures that errors from finite squeezing acting on encoded qubits are below the fault-tolerance threshold of known qubit-based error-correcting codes.[44]

The general process of QEC for QC and quantum communication is shown in Figs. 5(a) and 5(b), respectively. As shown in Fig. 5(a), in the QEC with stabilizer codes,[97] the encoded logical state $|\psi\rangle_{\rm L}$ is subject to an error process. Next, the code stabilizers are measured and the results are copied to a register of ancilla states $|A\rangle^{\otimes m}$. The ancilla states are then read out to give the syndrome result S. In the decoding process, the syndrome result is used to determine the best recover operation to correct the errors. As shown in Fig. 5(b), in the QEC for quantum communication, an input state $|\psi\rangle_{\rm in}$ and a set of ancillary states are encoded into a QEC code by the encoding circuit. The QEC code is transmitted through quantum channels where errors are introduced due to the noise in the environment. After the decoding circuit, the decoded ancillary states are used to identify the type and position of the error. By implementing a suitable error correction procedure based on the information in the syndrome procedure, the error will be corrected.

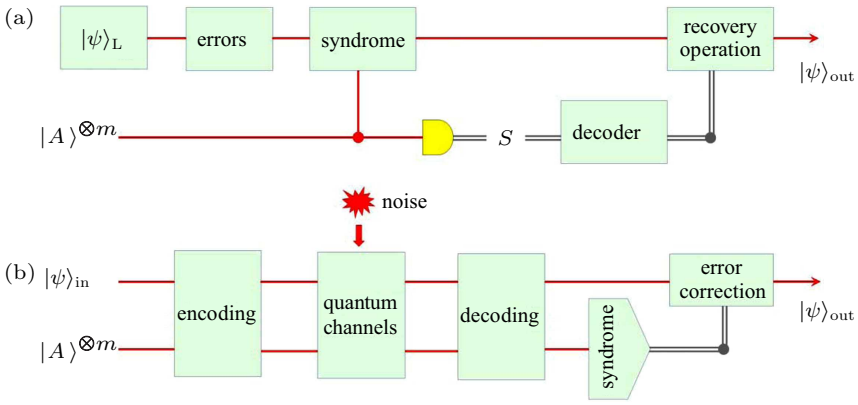

Fig. 5. The general process of QEC. (a) The QEC for errors in QC with stailizer codes. (b) The QEC for errors in quantum communication.

4.1. CV QEC with five-wave-packet code

Here, we take the example of CV QEC with five-wave-packet code to show the concrete QEC procedure in quantum communication.[95] This five-wave-packet belongs to the QEC code $[n,k,d]=[5,1,3]$, where $n=5$ denotes the number of used wave packets, $k=1$ is the number of logical encoded input state, and $d=3$ is the distance, which indicates how many errors can be tolerated, a code of distance d can correct up to $(d-1)/2$ arbitrary errors at unspecified channels. The schematic of the QEC with five-wave-packet code is shown in Fig. 6, which contains five steps. (1) Encoding. The input state is coupled with four auxiliary squeezed states using a beam-splitter network consisting of four beam-splitters. The encoded five modes is a five-mode CV linear cluster entangled state as shown in Fig. 6(a). (2) Error channel. The noise is randomly coupled into any one of the encoded five wave

packets. (3) Decoding. The decoding circuit is the inverse of the encoding circuit, which also contains four beam-splitters. (4) Syndrome recognition. Measuring the decoded auxiliary modes by homodyne detectors. The error in different channels results in different outputs of the homodyne detectors, which is used to identify the position of the error. (5) Error correction. Feedingfoward the corresponding measurement results of homodyne detectors to the output mode by the EOMs according to the error syndrome results.

After the error correction, single displacement error in phase space caused by channel noise is corrected. In this CV QEC experiment, the information of the input state is only distributed on three of the five channels and thus any error appearing in the remained two channels never affects the output state, i.e., the output quantum state is immune from the error in the two channels. The stochastic error on a single channel is corrected for both vacuum and squeezed input states and the achieved fidelities of the output states are beyond the corresponding classical limit.

Topological code is a special stabilizer QEC code whose generators are local but logical operators are topologically nontrivial and nonlocal.[98] Errors can be detected by measuring stabilizer operators. CV topological codes require new features such as the direction of edges, signs for anyonic charges, and more complicated string operators, such as fusion rules, and braiding rules.[98] In addition, some other concepts related to it have been proposed in recent years, such as the CV anyon statistics,[76] the graphical calculus for CV states[99] and its application in quantum communication,[100] the CV QC with anyons,[101] the exploration of CV fault-tolerant QC,[102] and topological entanglement entropy.[103]

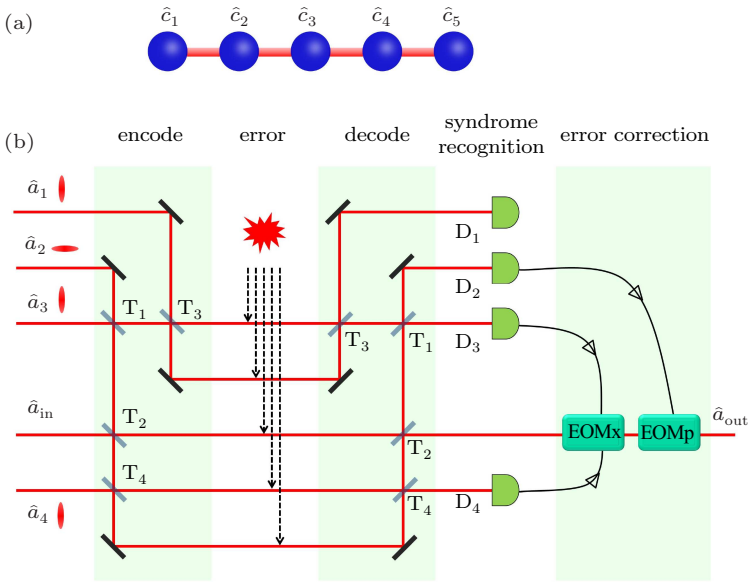

Fig. 6. The schematic of CV QEC with five-wave-packet code. (a) The graph representation of the five-wave-packet code. The input state is encoded on submodes $\hat{c}_3$, $\hat{c}_4$, and $\hat{c}_5$ of a five-partite linear cluster state $\hat{c}_{1-5}$. (b) The schematic of experimental set-up. EOM: electro-optical modulator, T_{1-4}: beam-splitters with 25%, 33%, 50%, and 50% transmission, respectively. D_{1-4}: homodyne detectors. Revised from Fig. 1 in Ref. [95].

4.2. CV QEC with correlated noisy channel

Noise is a main obstacle for the realization of CV quantum information processing. It has been shown that the noise in today's communication system exhibits correlations in time and space, thus it will be relevant to consider channels with a correlated noise.[104–106] In 2013, Lassen *et al.* experimentally realized CV QEC in a correlated noisy channel, in which a communication protocol relying on simple linear optics that optimally protects quantum states from correlated noise (non-Markovian) was proposed.[96] This QEC scheme protects arbitrary quantum states in a noisy non-Markovian environment by establishing a correlated Gaussian noisy channel. Using a simple linear optical encoding and decoding scheme, the near-ideal protection of coherent and entangled states from a highly noisy environment was demonstrated.

In 2016, Deng *et al.* experimentally demonstrated the disappearance and revival of the squeezing in quantum communication with squeezed state by using a correlated noisy channel.[107] In 2017, the disentanglement and the entanglement revival of a tripartite entangled state were also experimentally demonstrated.[108] Disentanglement is observed when the excess noise exists in the quantum channel. By creating a correlated noisy channel, entanglement of the tripartite entangled state is preserved, thus disentanglement can be avoided with the correlated noisy channel.

4.3. Fault-tolerant architecture

It has been shown that fault-tolerant linear optical quantum computing can be realized using two coherent states as a qubit basis.[102] Noiseless linear amplification (NLA) is the key operation to correct the error introduced by Gaussian noise.[109] In 2011, Ralph proposed a CV QEC protocol that

can correct the Gaussian noise induced by linear loss on Gaussian states.[110] This protocol is based on CV quantum teleportation and heralded NLA, which can be implemented by using linear optics and photon counting. A probabilistic NLA was experimentally demonstrated to amplify coherent states at the highest levels of effective gain based on a sequence of photon addition and subtraction.[111] It has also been shown that measurement-based NLA, which is equivalent to the heralding NLA, can be implemented by performing a post-selective filtering on the measurement results.[112]

The non-Gaussian operations are critical to fault tolerance of CV QC. The hybrid approach that takes advantage of both deterministic CV operations and robust qubit encoding becomes a trend in CV QEC.[66,86] Many different encoding schemes for CV QEC have been proposed such as GKP code,[66] encoding in cat states[102] and binomial states.[113,114] For these codes, a qubit is encoded on a square lattice in phase-space in a way that allows for the suppression of relevant errors (such as loss) to a certain extend.[115] Concatenating the GKP code with other qubit error correction code, for example toric GKP code,[86] surface-GKP code,[116] and the non-Gaussian oscillator-into-oscillators code,[117] provides a feasible method to correct general errors. It has been shown that initial squeezing in the cluster state above a threshold value of 20.5 dB ensures that errors from finite squeezing acting on encoded qubits are below the fault-tolerance threshold of known qubit-based error-correcting codes, which is a necessary condition for fault-tolerant measurement-based CV QC.[44]

5. Discussion and conclusion

Tremendous progress has been made in CV QC and QEC in recent years, as we reviewed in this manuscript. However, there are still some challenges for realization of universal and practical CV QC. Firstly, the cubic phase gate, which is a necessary quantum gate for universal CV QC, still remains a challenge although several proposals have been presented. Secondly, fault-tolerant CV QC is another challenge which is worth of further study. Thirdly, toward practical QC, it is essential to develop integrated quantum chips that include quantum source, circuits, and detectors for CV system. For example, CV chips for entangled state[118,119] and squeezed state[120–123] have been demonstrated, which demonstrate the feasibility of integrated quantum chips for CV system.

In summary, we briefly reviewed the progress of measurement-based CV QC and QEC, including the theoretical proposals and experimental demonstrations. We also discussed the fault-tolerant structure of CV QC and challenges ahead for realization of universal and practical CV QC. As the large scale CV cluster state in time domain has been achieved, it provides sufficient quantum resource for CV QC. Since non-Gaussian operation is required for universal measurement-based CV QC, it is essential to develop hybrid quantum information processing system that combines both DV and CV systems.[124]

References

[1] Shor P W 1994 *Proceedings 35th Annual Symposium on Foundations of Computer Science* November 20–22, 1994, Santa Fe, American
[2] Feynman R P 1982 *Int. J. Theor. Phys.* **21** 467
[3] Gambetta J M, Chow J M and Steffen M 2017 *npj Quantum Inf.* **3** 2
[4] Huang H L, Wu D, Fan D and Zhu X 2020 *Sci. China Inf. Sci* **63** 180501
[5] Li Z Y, Yu H F, Tan X S, Zhao S P and Yu Y 2019 *Chin. Phys. B* **28** 098505
[6] Brown K R, Kim J and Monroe C 2016 *npj Quantum Inf.* **2** 16034
[7] Zwanenburg F A, Dzurak A S, Morello A, Simmons M Y, Hollenberg L C L, Klimeck G, Rogge, Coppersmith S N and Eriksson M A 2013 *Rev. Mod. Phys.* **85** 961
[8] Nielsen M A and Chuang I L 2000 *Quantum Computation and Quantum Information* (Cambridge: Cambridge University Press) p. 287
[9] Raussendorf R and Briegel H J A 2001 *Phys. Rev. Lett.* **86** 5188
[10] Menicucci N C, van Loock P, Gu M, Weedbrook C, Ralph T C and Nielsen M A 2006 *Phys. Rev. Lett.* **97** 110501
[11] Walther P, Resch K J, Rudolph T, Schenck E, Weinfurter H, Vedral V, Aspelmeyer M and Zeilinger A 2005 *Nature* **434** 169
[12] Prevedel R, Walther P, Tiefenbacher F, Böhi P, Kaltenbaek R, Jennewein T and Zeilinger A 2007 *Nature* **445** 65
[13] Chen K, Li C M, Zhang Q, Chen Y A, Goebel A, Chen S, Mair A and Pan J W 2007 *Phys. Rev. Lett.* **99** 120503
[14] Lanyon B P, Jurcevic P, Zwerger M, Hempel C, Martinez E A, Dür W, Briegel H J, Blatt R and Roos R F 2013 *Phys. Rev. Lett.* **111** 210501
[15] Devoret M H and Schoelkopf R J 2013 *Science* **339** 1169
[16] Schindler P, Barreiro J T, Monz T, Nebendahl V, Nigg D, Chwalla M, Hennrich M and Blatt R 2011 *Science* **332** 1059
[17] Reed M D, Dicarlo L, Nigg S E, Sun L, Frunzio L, Girvin S M and Schoelkopf R J 2012 *Nature* **482** 382
[18] Arute F, Arya K, Babbush R, *et al.* 2019 *Narure* **574** 505
[19] Zhong H S, Wang H, Deng Y H *et al.* 2020 *Science* **370** 1460
[20] Braunstein S L and van Loock P 2005 *Rev. Mod. Phys.* **77** 513
[21] Weedbrook C, Pirandola S, García-Patrón R, Cerf N J, Ralph T C, Ahapiro J H and Lloyd S 2012 *Rev. Mod. Phys.* **84** 621
[22] Su X, Jia X, Zhang J, Xie C and Peng K 2007 *Phys. Rev. Lett.* **98** 070502
[23] Yukawa M, Ukai R, van Loock P and Furusawa A 2008 *Phys. Rev. A* **78** 012301
[24] Tan A, Wang Y, Jin X, Su X, Jia X, Zhang J, Xie C and Peng K 2008 *Phys. Rev. A* **78** 013828
[25] Su X L, Zhao Y P, Hao S H, Jia X, Xie C and Peng K 2012 *Opt. Lett.* **37** 5178
[26] Chen M, Menicucci N C and Pfister O 2014 *Phys. Rev. Lett.* **112** 120505
[27] Yokoyama S, Ukai R, Armstrong S C, Sornphiphatphong C, Kaji T, Suzuki S, Yoshikawa J I, Yonezawa H, Menicucci N C and Furusawa A 2013 *Nat. Photon.* **7** 982
[28] Yoshikawa J I, Yokoyama S, Kaji T, Sornphiphatphong C, Shiozawa Y, Makino K and Furusawa A 2016 *APL Photon.* **1** 060801
[29] Asavanant W, Shiozawa Y, Yokoyama S, Charoensombutamon B, Emura H, Alexander R N, Takeda S, Yoshikawa J, Menicucci N C, Yonezawa H and Furusawa A 2019 *Science* **366** 373
[30] Larsen M V, Guo X, Breum C R, Neergaard-Nielsen J S and Andersen U L 2019 *Science* **366** 369
[31] van Loock P, Weedbrook C and Gu M 2007 *Phys. Rev. A* **76** 032321
[32] Gu M, Weedbrook C, Menicucci N C, Ralph T C and van Loock P 2009 *Phys. Rev. A* **79** 062318
[33] Yoshikawa J I, Miwa Y, Huck A, Andersen U L, van Loock P and Furusawa A 2008 *Phys. Rev. Lett.* **101** 250501
[34] Miwa Y, Yoshikawa J I, van Loock P and Furusawa A 2009 *Phys. Rev. A* **80** 050303
[35] Wang Y, Su X, Shen H Tan A, Xie C and Peng K 2010 *Phys. Rev. A* **81** 022311
[36] Ukai R, Iwata N, Shimokawa Y, Armstrong S C, Politi A, Yoshikawa J I, van Loock P and Furusawa A 2011 *Phys. Rev. Lett.* **106** 240504

[37] Ukai R, Yokoyama S, Yoshikawa J I, van Loock P and Furusawa A 2011 *Phys. Rev. Lett.* **107** 250501
[38] Chiaverini J, Leibfried D, Schaetz T, Barrett M D, Blakestad R B, Britton J, Itano W M, Jost J D, Knill E, Langer C, Ozeri R and Wineland D J 2004 *Nature* **432** 602
[39] Yao X C, Wang T X, Chen H Z, Gao W B, Fowler A G, Raussendorf R, Chen Z B, Liu N L, Lu C Y, Deng Y J, Chen Y A and Pan J W 2012 *Nature* **482** 489
[40] Waldherr G, Wang Y, Zaiser S, Jamali M, Schulte-Herbrüggen T, ABe H, Ohshima T, Isoya J, Du J F, Neumann P and Wrachtrup J 2014 *Nature* **506** 204
[41] Kelly J, Barends R and Fowler A G 2015 *Nature* **519** 66
[42] Gottesman D 2010 *Proc. Symp. Appl. Math.* **68** 13
[43] Paler A and Devitt S J 2015 arXiv:1508.03695v1
[44] Menicucci N C 2014 *Phys. Rev. Lett.* **112** 120504
[45] Zhang J and Braunstein S L 2006 *Phys. Rev. A* **73** 032318
[46] Su X, Wang M, Yan Z, Jia X, Xie C and Peng K 2020 *Science China Information Sciences* **63** 180503
[47] Wang Y, Tian C, Su Q, Wang M and Su X 2019 *Science China Information Sciences* **62** 72501
[48] Briegel H J and Raussendorf R 2001 *Phys. Rev. Lett.* **86** 910
[49] Pysher M, Miwa Y, Shahrokhshahi R, Bloomer R and Pfister O 2011 *Phys. Rev. Lett.* **107** 030505
[50] Cai Y, Roslund J, Ferrini G, Arzani F, Xu X, Fabre C and Treps N 2017 *Nat. Commun.* **8** 15645
[51] Fukui K, Asavanant W and Furusawa A 2020 *Phys. Rev. A* **102** 032614
[52] van Loock P, Weedbrook C and Gu M 2007 *Phys. Rev. A* **76** 032321
[53] Bartlett S D, Sanders B C, Braunstein S L and Nemoto K 2002 *Phys. Rev. Lett.* **88** 097904
[54] Furusawa A and van Loock P 2011 *Quantum Teleportation and Entanglement: A Hybrid Approach to Optical Quantum Information Processing* (Hoboken: Wiley) p. 58
[55] Lloyd S and Braunstein S L 1999 *Phys. Rev. Lett.* **82** 1784
[56] Ukai R, Yoshikawa J I, Iwata N, van Loock P and Furusawa A 2010 *Phys. Rev. A* **81** 032315
[57] Adesso G and Illuminati F 2007 *J. Phys. A: Math. Theor.* **40** 7821
[58] Hao S, Deng X, Su X, Jia X, Xie C and Peng K 2014 *Phys. Rev. A* **89** 032311
[59] Marshall K, Jacobsen C, Schäfermeier C, Gehring T, Weedbrook C and Andersen U L 2016 *Nat. Commun.* **7** 13795
[60] Hao S H, Huang X S and Wang D 2017 *Chin. Phys. Lett.* **34** 070301
[61] Wang Y and Su Q 2017 *Chin. Phys. Lett.* **34** 070302
[62] Zhao J, Liu K, Jeng H, Gu M, Thompson J, Lam P K and Assad S M 2020 *Nat. Photon.* **14** 306
[63] Su X, Hao S, Deng X, Ma L, Wang M, Jia X, Xie C and Peng K 2013 *Nat. Commun.* **4** 2828
[64] Kumar R, Barrios E, Kupchak C and Lvovsky A I 2013 *Phys. Rev. Lett.* **110** 130403
[65] Parigi V, Zavatta A, Kim M and Bellini M 2007 *Science* **317** 1890
[66] Gottesman D, Kitaev A and Preskill J 2001 *Phys. Rev. A* **64** 012310
[67] Marek P and Filip R 2011 *Phys. Rev. A* **84** 053802
[68] Marshall K, Pooser R Siopsis G and Weedbrook C 2015 *Phys. Rev. A* **91** 032321
[69] Miyata K, Ogawa H, Marek P, Filip R, Yonezawa H, Yoshikawa J I and Furusawa A 2016 *Phys. Rev. A* **93** 022301
[70] Yukawa M, Miyata K, Yonezawa H, Marek P, Filip R and Furusawa A 2013 *Phys. Rev. A* **88** 053816
[71] Lloyd S 1996 *Science* **273** 1073
[72] Buluta I and Nori F 2009 *Science* **326** 108
[73] Cirac J I and Zoller P 2012 *Nat. Phys.* **8** 264
[74] Georgescu I M, Ashhab S and Nori F 2014 *Rev. Mod. Phys.* **86** 153
[75] Ghose S and Sanders B C 2007 *J. Mod. Opt.* **54** 855
[76] Zhang J, Xie C, Peng K and van Loock P 2008 *Phys. Rev. A* **78** 052121
[77] Marshall K, Pooser R, Siopsis G and Weedbrook C 2015 *Phys. Rev. A* **92** 063825
[78] Huh J, Guerreschi G, Peropadre B, McClean J R and Aspuru-Guzik A 2015 *Nat. Photon.* **9** 615
[79] Arrazola J M and Bromley T R 2018 *Phys. Rev. Lett.* **121** 030503
[80] Brádler K, Dallaire-Demers P L, Rebentrost P, Su D and Weedbrook C 2018 *Phys. Rev. A* **98** 032310
[81] Deng X, Hao S, Guo H, Xie C and Su X 2016 *Sci. Rep.* **6** 22914
[82] Sefi S and van Loock P 2011 *Phys. Rev. Lett.* **107** 170501
[83] Sudhir V, Genoni M G, Lee J and Kim M S 2012 *Phys. Rev. A* **86** 012316
[84] Braunstein S L 1998 *Phys. Rev. Lett.* **80** 4084
[85] Lloyd S and Slotine J J E 1998 *Phys. Rev. Lett.* **80** 4088
[86] Vuillot C, Asasi H, Wang Y, Pryadko L P and Terhal B M 2019 *Phys. Rev. A* **99** 032344
[87] Niset J, Fiurášek J and Cerf N J 2009 *Phys. Rev. Lett.* **102** 120501
[88] Dong R, Lassen M, Heersink J, Marquardt C, Filip R, Leuchs G and Andersen U L 2008 *Nat. Phys.* **4** 919
[89] Hage B, Samblowski A, DiGuglielmo J, Franzen A, Fiurášek J and Schnabel R 2008 *Nat. Phys.* **4** 915
[90] Braunstein S L 1998 *Nature* **394** 47
[91] Walker T A and Braunstein S L 2010 *Phys. Rev. A* **81** 062305
[92] Wilde M M, Krovi H and Brun T A 2007 *Phys. Rev. A* **76** 052308
[93] Niset J, Andersen U L and Cerf N J 2008 *Phys. Rev. Lett.* **101** 130503
[94] Aoki T, Takahashi G, Kajiya T, Yoshikawa J I, Braunstein S L, van Loock P and Furusawa A 2009 *Nat. Phys.* **5** 541
[95] Hao S, Su X, Tian C, Xie C and Peng K 2015 *Sci. Rep.* **5** 15462
[96] Lassen M, Berni A, Madsen L S, Filip R and Andersen U L 2013 *Phys. Rev. Lett.* **111** 180502
[97] Roffe J 2019 *Contemporary Phys.* **60** 226
[98] Morimae T 2013 *Phys. Rev. A* **88** 042311
[99] Menicucci N C, Flammia S T and van Loock P 2011 *Phys. Rev. A* **83** 042335
[100] Menicucci N C, Baragiola B Q, Demarie T F and Brennen G K 2018 *Phys. Rev. A* **97** 032345
[101] Milne D F, Korolkova N V and van Loock P 2012 *Phys. Rev. A* **85** 052325
[102] Lund A P, Ralph T C and Haselgrove H L 2008 *Phys. Rev. Lett.* **100** 030503
[103] Demarie T F, Linjordet T, Menicucci N C and Brennen G K 2014 *New J. Phys.* **16** 085011
[104] Maniscalco S, Olivares s and Paris M G A 2007 *Phys. Rev. A* **75** 062119
[105] Vasile R, Olivares S, Paris M G A and Maniscalco S 2009 *Phys. Rev. A* **80** 062324
[106] Weedbrook C, Pirandola S, Garcí-Patrón R on, Cerf N J, Ralph T C, Shapiro J H and Lloyd S 2012 *Rev. Mod. Phys.* **84** 621
[107] Deng X, Hao S, Tian C, Su X, Xie C and Peng K 2016 *Appl. Phys. Lett.* **108** 081105
[108] Deng X, Tian C, Su X and Xie C 2017 *Sci. Rep.* **7** 44475
[109] Ralph T C and Lund A P 2009 *AIP Conference Proceedings* **1110** 155
[110] Ralph T C 2011 *Phys. Rev. A* **84** 022339
[111] Zavatta A, Fiurášek J and Bellini M A 2011 *Nat. Photon.* **5** 52
[112] Chrzanowski H, Walk N, Assad S M, Janousek J, Hosseini S, Ralph T C, Symul T and Lam P K 2014 *Nat. Photon.* **8** 333
[113] Michael M H, Silveri M, Brierley R T, Albert V V, Salmilehto J, Jiang L and Girvin S M 2016 *Phys. Rev. X* **6** 031006
[114] Albert V V, Noh K, Duivenvoorden K, Youn D J, Brierley R T, Reinhold P, Vuillot C, Li L, Shen C, Girvin S M, Terhal B M and Jiang L 2018 *Phys. Rev. A* **97** 032346
[115] Larsen M V, Neergaard-Nielsen J S and Andersen U L 2020 arXiv: 2005.13513v1
[116] Noh K and Chamberland C 2020 arXiv: 1908.03579v2
[117] Noh K, Girvin S M and Jiang L 2020 arXiv: 1903.12615v3
[118] Masada G, Miyata K, Politi A, Hashimoto T, O'Brien J L and Furusawa A 2015 *Nat. Photon.* **9** 316
[119] Lenzini F, Janousek J, Thearle O, Villa1 M, Haylock B, Kasture1 S, Cui L, Phan H P, Dao D V, Yonezawa H, Lam P K, Huntington E H and Lobino M 2018 *Sci. Adv.* **4** eaat9331
[120] Dutt A, Luke K, Manipatruni S, Gaeta A L, Nussenzveig P and Lipson M 2015 *Phys. Rev. A* **3** 044005
[121] Dutt A, Miller S, Luke K, Gardenas J, Gaeta A L, Nussenzveig P and Lipson M 2016 *Opt. Lett.* **41** 223
[122] Otterpohl A, Sedlmeir F, Vogl U, Dirmeier T, Shafiee G, Schunk G, Strekalov D V, Schwefel H G L, Gehring T, Andersen U L, Leuchs G and Marquardt G 2019 *Optica* **6** 1375
[123] Zhao Y, Okawachi Y, Jang J K, Ji X, Lipson M and Gaeta A L 2020 *Phys. Rev. Lett.* **124** 193601
[124] Andersen U L, Neergaard-Nielsen J S, van Loock P and Furusawa A 2015 *Nat. Phys.* **11** 713